

On methods of estimating stability of braced excavations in clay

Tuan Nghia Do¹

¹ Faculty of Civil Engineering, Thuyloi University, 175 Tayson Street, HAN, Vietnam.

ABSTRACT

In this paper, four methods of estimating stability of braced excavations in clay, including the load factor (push-in gross pressure) method, the strength factor method, the slip circle method, and the finite element method (FEM) with reduced shear strength were compared. The struts, center posts, and walls of the bracing systems were modelled with elastoplastic behaviors. During the variation of the undrained shear strength (s_u) of soil, the ratio between wall embedded depth to excavation depth (H_p/H_e) was determined in order to obtain the factors of safety of excavations estimated by the above methods at 1.2. It could be observed from results that when s_u was constant with depth, the load factor method gave two H_p/H_e values corresponding to each s_u value, which was unreasonable. If the constant s_u value was increased, the H_p/H_e values by the strength factor method and slip circle method would be larger than those by FEM as $\gamma H_e/s_u \leq 4.5$ but smaller as $\gamma H_e/s_u > 4.5$ (γ was unit weight of soil). When s_u/σ_v' was constant with depth, the H_p/H_e values by the load factor method, the strength factor method, and slip circle method would be greater than those by FEM as $\gamma H_e/s_u \leq 7.0$ but smaller as $\gamma H_e/s_u > 7.0$ (s_u was taken at the excavation bottom). In general, the strength factor method and the slip circle method generated the most reasonable results as compared with FEM. Case histories were also employed to validate results of the methods.

Keywords: Deep excavations; Stability analysis; Finite element method.

1 INTRODUCTION

So far, the load factor and the strength factor methods have been often recommended by CIRIA report 104 (Padfield and Mair, 1984) and BS 8002 (British Standard Institute, 1994) for estimating stability of an embedded retaining wall. On the other hand, the slip circle method has been widely employed to estimate stability of excavations in clay in most of Asian countries. The method is advocated by TGS (Taiwanese Geotechnical Society 2001) and JSA (Japanese Society Architecture 1988). Very recently, the finite element method (FEM) with reduced shear strength has been significantly improved to analyze the stability of braced excavations. The method has many advantages over the conventional hand-calculation ones, i.e. the failure surface of soil comes out naturally without any assumptions, etc. Do et al. (2016) demonstrated that the method in associated with modelling an elastoplastic support system was capable of predicting failure mechanism of real excavation cases in clay. Also, stability of excavations, which was strongly related to that of walls, could be estimated using the method.

In this study, the load factor method, the strength factor method, and the slip circle method, which are widely used hand calculation methods, will be examined in estimating stability of wide excavations in clay. Excavations were retained by the wall with multiprop levels. The variations of normalized undrained shear strength (s_u/σ_v') and undrained shear strength (s_u) values were taken into account. Results of the above three

methods were compared to those from the FEM with reduced shear strength and consideration of the elastoplastic behavior of the support system. The results from the FEM was treated as the standard method referring the study by Do et al. (2016). A large number of failure and successful excavations in clay were also adopted for further validation.

2 METHODOLOGY

2.1 Load factor method and strength factor method

The methods were originally established for the wall with one prop level. In this study, they would be extended for the multipropped wall.

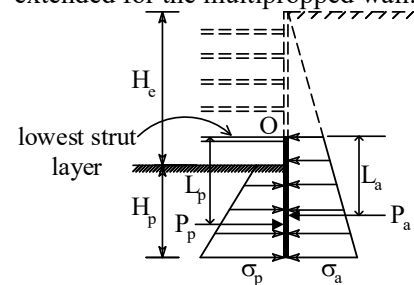


Fig. 1. Load factor and strength factor methods.

The load factor method estimates the stability of the wall under effects of lateral earth pressures in the active and passive zones. Considering the short-term behavior of the subsoil (saturated clay), these extreme earth pressures are calculated as follows:

$$\sigma_a = \sigma_v - 2s_u\sqrt{1 + c_w/s_u} \quad (1)$$

$$\sigma_p = \sigma_v + 2s_u\sqrt{1 + c_w/s_u} \quad (2)$$

where σ_a and σ_p = active and passive earth pressures, respectively; σ_v = overburden pressure; s_u = undrained shear strength of soil; c_w = adhesion between wall and soil.

As shown in Fig. 1, this method takes into account the wall part from the lowest strut level to the wall toe in equilibrium analysis. The factor of safety of stability (F_{LF}) is calculated using the following equation:

$$F_{LF} = P_p L_p / P_a L_a \quad (3)$$

where P_p and P_a = resultant forces of the passive and active earth pressures, respectively; L_p and L_a = distance from the lowest strut level to the acting point of P_p and P_a , respectively;

The strength factor method considers stability of the same wall part but defines the maximum coefficient applied to reduce soil strength at which equilibrium state remains as the factor of safety (F_{SF}):

$$F_{SF} = s_{u,org} / s_{u,lim} \quad (4)$$

where $s_{u,org}$ and $s_{u,lim}$ = undrained shear strength of soil at the beginning and the limiting equilibrium state, respectively.

2.2 Slip circle method

The slip circle method is performed using the following procedure: (1) assume a trial circular failure surface; (2) calculate the ratio of the resistant moment to the driving moment; (3) repeat steps (1) and (2) until the smallest ratio is obtained. Then, the method will treat the smallest ratio as the factor of safety (F_{SC}) and the corresponding surface as the failure surface of the excavation. Since the failure surface often centers at the lowest strut level, one of the trial surfaces can be observed in Fig. 2. The ratio of the resistant moment to the driving moment is calculated as follows:

$$\frac{M_r}{M_d} = \frac{R \int_0^{(\frac{\pi}{2})+\alpha} s_u(Rd\theta)}{W(\frac{R}{2})} = \frac{\int_0^{(\frac{\pi}{2})+\alpha} s_u(Rd\theta)}{W/2} \quad (5)$$

where R = radius of the trial surface; s_u = undrained shear strength of soil; W = self-weight of the soil body within the DEFG area.

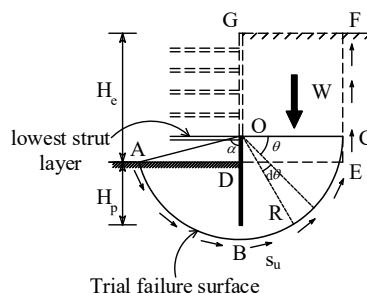


Fig. 2. Slip circle method.

2.3 FEM with reduced shear strength

The FEM with reduced shear strength makes use of the computer program to estimate the stability of the

excavation. It follows that the strength parameters of soil will be reduced constantly until numerical solutions diverge. Divergence of numerical solutions is defined as failure of the excavation and the maximum SR ratio is the factor of safety (FEM) of the excavation. Details of the method can be seen elsewhere, e.g. Do et al. (2016).

2.4 Excavation geometry, construction sequence, and soil profile

Fig. 3 plots the excavation geometry used in this study, which was the popular one in practice. The final excavation depth was 18 m and reached within six stages. The excavation width was assumed to be very large (i.e., 150 m) in order to avoid the overlapping effect of the failure surfaces of soil below the excavation bottom. The subsoil was a thick deposit of clay so that the influence of the hard stratum was eliminated. The ground water table was located on the ground surface.

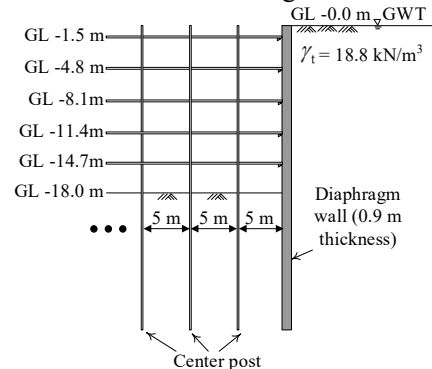


Fig. 3. Excavation geometry

As shown in Fig. 3, the support system was composed of a 0.9-m-thick diaphragm wall and five levels of horizontal struts. It was assumed that the horizontal spacing of struts was 6 m and that of center posts was 5 m. Dimensions of the structural elements used to support the typical excavations was summarized in Table 1. Details of the selection of the structural elements were described in the study by Do (2016).

Table 1. Dimensions of structural elements

Strut layer	$s_u/\sigma_v' = \text{const}$			$s_u = \text{const (kPa)}$		
	0.18	0.22	0.30	70	80	90
1	H350	H350	H350	H250	H200	H200
2	4H250	2H350	2H350	H350	H350	H350
3	2H400	4H250	2H350	H350	H350	H350
4	2H400	4H250	2H350	H350	H350	H350
5	2H400	4H250	2H350	H350	H350	H300
Center post	H350	H350	H350	H250	H200	H200
Wall thickness (m)	0.9					

Note: H200, H250, H300, H350, and H400 denote H200x200x8x12, H250x250x9x14, H300x300x10x15, H350x350x12x19, H400x400x13x21, respectively.

Effects of wall embedded depth and wall friction were studied by varying H_p/H_e (wall embedded depth/excavation depth) and c_w/s_u , respectively. To

examine the effects of the undrained shear strength of soil, the s_u/σ_v' ratio was varied. The excavations were modelled according to the way described by Do (2016).

3 RESULTS AND DISCUSSION

3.1 $s_u = \text{const}$

Fig. 4 plots the variation of H_p/H_e ratios determined by the four methods for different s_u values. For a given s_u value, H_p/H_e is separately determined by these methods in order to have the corresponding factor of safety equal to 1.2. The factor of safety of 1.2 was selected based on the fact that this number has been broadly adopted by practicing engineers for stability of excavations, especially in Japan and Taiwan. In addition, the stability number, N_b , is employed to roughly indicate stability of excavation. N_b is calculated as follows: $N_b = \gamma H_e / s_u$ where γ = unit weight of soil; H_e = excavation depth; s_u = undrained shear strength of soil between the excavation bottom and the influenced depth of excavation. When s_u reduces from 92 kPa to 68 kPa ($N_b = 3.7$ to 5.0), $H_p/H_{e, \text{FEM}}$ increases rapidly with s_u . It is due to the fact that the wall cannot retain well the soil behind from moving toward the excavation as shown in Fig. 5 for a typical case so that a small decrease in the soil strength will require the large increase in the wall embedded depth (or $H_p/H_{e, \text{FEM}}$) to remain the factor of safety at 1.2.

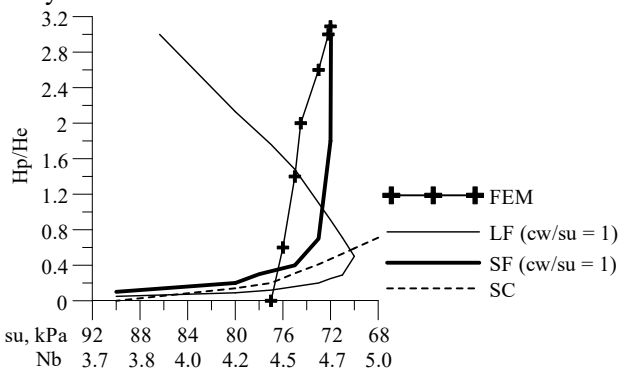


Fig. 4. H_p/H_e estimated by different methods at factor of safety of 1.2 ($s_u = \text{const}$)

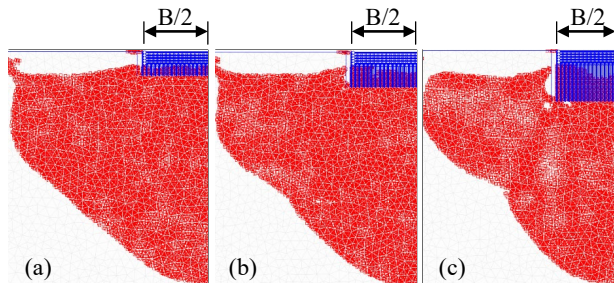


Fig. 5. Plastic point plots just before failure of excavation as $s_u = 75$ kPa and: (a) $H_p/H_e = 0.6$; (b) $H_p/H_e = 1.4$; and (c) $H_p/H_e = 2.6$

Also shown in Fig. 4, $H_p/H_{e, \text{SC}}$ steadily increases with the decrease of s_u . $H_p/H_{e, \text{SC}}$ increases gently when $s_u \geq 76$ kPa ($N_b \leq 4.5$) and significantly when $s_u < 76$ kPa (N_b

> 4.5). $H_p/H_{e, \text{SC}}$ is close to $H_p/H_{e, \text{SF}}$ as $s_u \geq 76$ kPa ($N_b \leq 4.5$) but smaller than $H_p/H_{e, \text{SF}}$ as $s_u < 76$ kPa ($N_b > 4.5$). On the other hand, results by the load factor method are not reasonable because this method generates two H_p/H_e ratios corresponding to a s_u value. As compared with results by the FEM, it can be seen that the strength factor method and the slip circle method overestimate the required H_p/H_e ratio as $s_u \geq 76$ kPa ($N_b \leq 4.5$) but underestimate the ratio as $s_u < 76$ kPa ($N_b > 4.5$).

3.2 $s_u/\sigma_v' = \text{const}$

Fig. 6 shows the comparison of H_p/H_e ratios determined by the load factor method ($H_p/H_{e, \text{LF}}$), the strength factor method ($H_p/H_{e, \text{SF}}$), the slip circle method ($H_p/H_{e, \text{SC}}$), and the FEM ($H_p/H_{e, \text{FEM}}$) for different s_u/σ_v' values. As shown in the figure, $H_p/H_{e, \text{FEM}}$ and s_u/σ_v' have the curved relationship. However, at the beginning, when s_u/σ_v' is small (i.e., $s_u/\sigma_v' = 0.22$), $H_p/H_{e, \text{FEM}}$ is highly sensitive to the change of s_u/σ_v' as indicated by the nearly vertical part of the curve in the figure. For a given excavation, the driving force caused by the volume of removed soil was constant. Since the factor of safety was fixed at 1.2, the required resistant force, which is equal to the driving force multiplied with the factor of safety, will be constant. The resistance force, on the other hand, was mobilized from the soil shear strength and the retaining capacity of the wall to prevent the surrounding soil from moving toward the excavation. In general, when s_u/σ_v' (or soil strength) reduces, $H_p/H_{e, \text{FEM}}$ needs to be increased to employ more the retaining capacity of the wall. Particularly, when s_u/σ_v' is large (i.e., $s_u/\sigma_v' > 0.22$), $H_p/H_{e, \text{FEM}}$ is often small (i.e., $H_p/H_{e, \text{FEM}} < 1.2$). As shown in Figs. 7a and 7b for a typical case, the extending of the wall embedded depth improved significantly the factor of safety because it retained effectively the soil movement toward the excavation zone. As a result, $H_p/H_{e, \text{FEM}}$ required to remain the factor of safety at 1.2 just increased slowly with s_u/σ_v' . When the s_u/σ_v' ratio was small, $H_p/H_{e, \text{FEM}}$ became large (i.e., $H_p/H_{e, \text{FEM}} \geq 1.2$ as $s_u/\sigma_v' \leq 0.22$). The increase in the wall embedded depth did not improve much the factor of safety because the mobilized resistance of soil as indicated by the radius of the failure surface (Figs. 7b and 7c) and the mobilized retaining capacity of wall as indicated by the number of plastic points on wall (Figs. 7b and 7c) kept constant with H_p/H_e . In order to remain the factor of safety at 1.2, $H_p/H_{e, \text{FEM}}$ needed to be increased largely with s_u/σ_v' as indicated by the vertical part of the curve in Fig. 6.

When s_u/σ_v' is increased from 0.16 to 0.36 ($N_b = 4.2 \div 9.5$), H_p/H_e calculated by all of the methods generally decreases. It is observed that $H_p/H_{e, \text{SF}}$ and $H_p/H_{e, \text{SC}}$ are very close to each other. $H_p/H_{e, \text{LF}}$ is greater than $H_p/H_{e, \text{SF}}$ and $H_p/H_{e, \text{SC}}$ as $s_u/\sigma_v' \leq 0.3$ ($N_b \geq 5.1$) but close to them as $s_u/\sigma_v' > 0.3$ ($N_b < 5.1$). The relationships between H_p/H_e by the three methods and s_u/σ_v' are generally smooth curves.

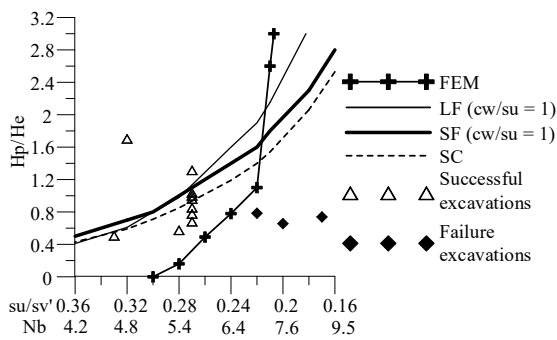


Fig. 6. H_p/H_e estimated by different methods at factor of safety of 1.2 ($s_u/\sigma_v' = \text{const}$)

As compared with H_p/H_e , FEM, which is considered as a standard value, the three hand-calculation methods would underestimate the required wall embedded depth (H_p/H_e) as $s_u/\sigma_v' \leq 0.22$ ($N_b \geq 7.0$) and overestimate the depth as $s_u/\sigma_v' > 0.22$ ($N_b < 7.0$).

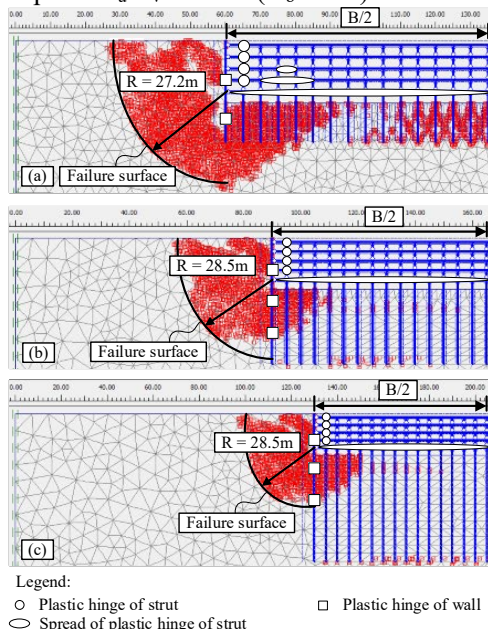


Fig. 7. Plastic point plots just before numerical failure of excavation as $s_u/\sigma_v' = 0.22$ and: (a) $H_p/H_e = 0.6$; (b) $H_p/H_e = 1.4$; and (c) $H_p/H_e = 2.6$

For validation, H_p/H_e ratios of case histories, including failure and successful excavations, are added into Fig. 6. As shown in the figure, the predicting curves of the four methods locate above the black points of the failure cases so that the required H_p/H_e ratios are greater than those adopted in the field. Therefore, failure of the cases, in view of the four methods, is reasonable. At the successful cases, the predicting curve of the FEM stays below the white points of the cases while those of the load factor method, the strength factor method, and the slip circle method lie among these points. Hence, these methods require the smaller or equivalent H_p/H_e ratios as compared with the real ones and also indicate the success in excavation of the cases.

4 CONCLUSIONS

In this study, the load factor method and the strength factor method (recommended by CIRIA report 104 and BS 8002) as well as the slip circle method (advocated by TGS, 2001 and JSA, 1988) have been investigated in estimating stability of wide excavations. The excavations are performed in a thick desposit of clay and supported by the wall with multiprop levels. Results of these methods are compared with those of the FEM, which is treated as the standard method (Do et al., 2016). On the basis of this study, some conclusions can be drawn as follows:

i. When s_u is constant, the required H_p/H_e ratios estimated by the slip circle method are close to those by the strength factor method as $s_u \geq 76$ kPa ($N_b \leq 4.5$) but smaller than them as $s_u < 76$ kPa ($N_b > 4.5$). As compared with the FEM, results of the strength factor method and the slip circle method are greater than those of the FEM as $s_u \geq 76$ kPa ($N_b \leq 4.5$) and smaller as $s_u < 76$ kPa ($N_b > 4.5$). The load factor method gives illogical results since it requires two different H_p/H_e ratios corresponding to each of s_u values.

ii. When s_u/σ_v' is constant, the strength factor method and the slip circle method always give similar H_p/H_e ratios. Results of the load factor method are close to those of the above methods as $s_u/\sigma_v' \geq 0.3$ ($N_b \leq 5.1$) but greater than them as $s_u/\sigma_v' < 0.3$ ($N_b > 5.1$). As compared with the FEM, the three hand-calculation methods will overestimate the H_p/H_e ratio as $s_u/\sigma_v' \geq 0.22$ ($N_b \leq 7.0$) but underestimate the ratio as $s_u/\sigma_v' < 0.22$ ($N_b > 7.0$). These four methods can predict the reasonable H_p/H_e ratios as validated by the real failure and successful excavations.

REFERENCES

- BS 8002 (British Standard Institute) (1994). Code of Practice for Earth Retaining Structures, London.
- Do, T. N., Ou, C. Y., and Chen, R. P. (2016). A Study of Failure Mechanisms of Deep Excavations in Soft Clay Using the Finite Element Method. *Computer and Geotechnics*, 153-163.
- Do, T. N. (2016). A Study of Stability of Deep Excavations in Clay with Consideration of A Full Elastoplastic Support System. PhD Dissertation, National Taiwan University of Science & Technology, Taipei, Taiwan, R.O.C.
- JSA (Japan Society of Architecture) (1988). Guidelines of Design and Construction of Deep Excavations, Tokyo.
- Padfield, C. J. and Mair, R. J. (1984). Design of Retaining Walls Embedded in Stiff Clays. CRIR Report No. 104, England, 83-84.
- TGS (Taiwanese Geotechnical Society) (2001). Design Specifications for the Foundation of the Building, Taipei, Taiwan, R.O.C.